DMD Fast Forward. Published on January 18, 2011 as doi:10.1124/dmd.110.037036
This article has not been copyedited and formatted. The final version may differ from this version.

DMD #37036

Characterization of niflumic acid as a selective inhibitor of human liver microsomal UDP-glucuronosyltransferase 1A9: Application to the reaction phenotyping of acetaminophen glucuronidation

John O Miners, Kushari Bowalgaha, David J. Elliot, Pawel Baranczewski and Kathleen M Knights

Department of Clinical Pharmacology, School of Medicine, Flinders University, Adelaide, Australia (JOM, KB, DJE, KMK)

Clinical Pharmacology and DMPK, AstraZeneca R & D Sodertalje, Sweden (PB)

Running title: UGT enzyme inhibition selectivity of niflumic acid

Address for correspondence:

Professor John O. Miners

Department of Clinical Pharmacology

Flinders University School of Medicine

Flinders Medical Centre

Bedford Park, SA 5042

Australia

Telephone: 61-8-82044131

Fax: 61-8-82045114

Email: john.miners@flinders.edu.au

Number of text pages: 36 (excluding tables)

Number of Figures: 8

Number of Tables: 3

Number of references: 41

Word count: Abstract, 250; Introduction, 743; Discussion, 1400.

Abbreviations: APAP, acetaminophen (N-acetyl-p-aminophenol); APAPG, acetaminophen β-D-glucuronide; AZT, zidovudine; β-E2, β-estradiol; COD, codeine; DEF, deferiprone; HLM, human liver microsomes; LTG, lamotrigine; 4MU, 4-methylumbelliferone; NFA, niflumic acid; PRO, propofol; TFP, trifluoperazine; TST, testosterone; UDPGA, UDP-glucuronic acid; UGT, UDP-glucuronosyltransferase

DMD Fast Forward. Published on January 18, 2011 as DOI: 10.1124/dmd.110.037036
This article has not been copyedited and formatted. The final version may differ from this version.

ABSTRACT

Enzyme selective inhibitors represent the most valuable experimental tool for reaction phenotyping. However, only a limited number of UDP-glucuronosyltransferase (UGT) enzyme selective inhibitors have been identified to date. This study characterized the UGT enzyme selectivity of niflumic acid (NFA). It was demonstrated that NFA, 2.5 μM, is a highly selective inhibitor of recombinant and human liver microsomal (HLM) UGT1A9 activity. Higher NFA concentrations (50 – 100 μM) inhibited UGT1A1 and UGT2B15, but had little effect on the activities of UGT1A3, UGT1A4, UGT1A6, UGT2B4, UGT2B7 and UGT2B17. NFA inhibited 4-methylumbelliferone and propofol (PRO) glucuronidation by recombinant UGT1A9 and PRO glucuronidation by HLM according to a mixed (competitive – non-competitive) mechanism, with K_i values ranging from 0.10 to 0.40 μM. Similarly, NFA was a mixed or non-competitive inhibitor of recombinant and human liver microsomal UGT1A1 (K_i range 14 to 18 μM), whereas competitive inhibition (K_i 62 μM) was observed with UGT2B15. NFA was subsequently applied to the reaction phenotyping of human liver microsomal acetaminophen (APAP) glucuronidation. Consistent with previous reports, APAP was glucuronidated by recombinant UGT1A1, UGT1A6, UGT1A9 and UGT2B15. NFA concentrations in the range 2.5 – 100 μM inhibited APAP glucuronidation by UGT1A1, UGT1A9 and UGT2B15, but not by UGT1A6. The mean V_{max} for APAP glucuronidation by HLM was reduced by 20%, 35% and 40%, respectively, in the presence of NFA 2.5, 50 and 100 μM. Mean K_m values decreased in parallel with V_{max}, although the magnitude of the decrease was smaller. Taken together, the NFA inhibition data suggest that UGT1A6 is the major enzyme involved in APAP glucuronidation.

INTRODUCTION

The importance of conjugation with glucuronic acid ('glucuronidation') as an elimination and detoxification mechanism for xenobiotics and endogenous compounds has become increasingly recognized over the last two decades. In particular, glucuronidation contributes to the clearance of structurally diverse drugs from all therapeutic classes (Kiang et al., 2005; Miners and Mackenzie, 1991). The glucuronidation reaction is catalyzed by UDP-glucuronosyltransferase (UGT) and, consistent with its broad substrate profile, UGT is known to exist as an enzyme 'superfamily' in humans. Eighteen human UGT proteins that utilize UDP-glucuronic acid as cofactor have been characterized to date and these have been classified in three subfamilies, UGT1A, UGT2A and UGT2B, based on amino acid sequence identity (Mackenzie et al., 2005). Of the eleven UGT proteins expressed to a significant extent in liver current evidence suggests that UGT 1A1, 1A4, 1A6, 1A9, 2B7 and 2B15 are of greatest importance in the hepatic metabolism of drugs, although UGT 1A3, 2B4 and 2B10 also contribute to drug glucuronidation (Kiang et al., 2005; Miners et al., 2010a).

While most human UGT enzymes glucuronidate low molecular mass aliphatic alcohols and phenols, enzyme substrate selectivity occurs with increasing structural complexity of the aglycone (Miners et al., 2006 and 2010a). Similarly, the individual enzymes tend to differ in terms of inhibitor selectivity and hence patterns of drug-drug interactions (Kiang et al., 2005, Miners et al., 2010b). Moreover, activities appear to be variably affected by age, alcohol consumption, cigarette smoking, diet, disease states, ethnicity, genetic polymorphism, and hormonal factors (Court et al., 2010; Guillemette 2003; Miners and Mackenzie, 1991; Miners et al., 2002 and 2004).

DMD Fast Forward. Published on January 18, 2011 as DOI: 10.1124/dmd.110.037036
This article has not been copyedited and formatted. The final version may differ from this version.

Given these features of human UGT enzymes, attention has focussed on the identification of enzyme-selective substrate and inhibitor probes for the reaction phenotyping of drug glucuronidation reactions. UGT enzyme selective substrates have been identified for the main human hepatic drug metabolizing UGTs and these may be employed in activity correlation studies in a panel of human liver microsomes (HLM) or hepatocytes (Court, 2005; Miners et al., 2006 and 2010a). However, enzyme selective inhibitors represent a more valuable experimental tool for reaction phenotyping since the extent of inhibition of the glucuronidation of a test compound by HLM or hepatocytes reflects the contribution of the individual UGT enzymes to metabolic clearance. In contrast to the ready availability of substrate probes, only two UGT enzyme selective inhibitors have been identified to date. Hecogenin (10 μM) is a highly selective inhibitor of UGT1A4 (Uchaipichat et al., 2006a) and fluconazole (2500 μM) is a moderately selective inhibitor of UGT2B7 (Uchaipichat et al., 2006b), although more recent studies suggest similar inhibition of UGT2B4 (Raungrut et al., 2010). (Isolongifolol and a phenyl substituted secondary alcohol derived from this compound have been reported to be potent, selective inhibitors of recombinant UGT2B7 (Bichlmaier et al., 2007), although experimental conditions for selective inhibition of human liver microsomal UGT2B7 appear not to have been characterized.)

While UGT1A1 appears to be the principal enzyme involved in the glucuronidation of the non-steroidal anti-inflammatory drug niflumic acid (NFA; Mano et al., 2006a), it has been demonstrated that this compound potently inhibits 4-methylumbelliferone (4MU) glucuronidation by recombinant UGT1A9 (Gaganis et al., 2007; Mano et al.,

2006b). In addition, it has been reported that NFA inhibits the glucuronidation of the predominantly UGT1A9 substrate mycophenolic acid with HLM as the enzyme source (Vietri et al., 2002). However, high concentrations of NFA may also inhibit other UGT enzymes (Gaganis et al., 2007). To investigate the potential utility of NFA as an inhibitor probe for the reaction phenotyping of drug glucuronidation reactions, this study characterized the concentration dependence of UGT enzyme inhibition by NFA and the mechanism of inhibition. The results demonstrated that, under appropriate experimental conditions, NFA selectively inhibits UGT1A9 and, to a lesser extent, UGT1A1 and UGT2B15.

Following demonstration of UGT enzyme selectivity, NFA inhibition was applied to the reaction phenotyping of acetaminophen (APAP; paracetamol) glucuronidation by HLM. Glucuronidation accounts for approximately 65% of the metabolic clearance of a therapeutic dose of APAP in humans (Miners et al., 1984). Although APAP is one of the most widely used drugs worldwide, the relative contribution of individual UGT enzymes to APAP glucuronidation is yet to be completely resolved. While APAP glucuronidation is generally attributed to UGT 1A1, 1A6 and 1A9 (Bock et al., 1993; Court et al., 2001), more recently Mutlib et al. (2006) proposed a significant role for UGT2B15. Thus, NFA inhibition was used here to further explore the relative contribution each of these enzymes to APAP glucuronidation by HLM.

MATERIALS AND METHODS

Materials

Acetaminophen β-D-glucuronide (APAPG), alamethicin (from *Trichoderma viride*), acetaminophen (APAP), codeine (COD), 4-methylumbelliferone (4MU), 4-methylumbelliferone β-D-glucuronide, β-estradiol (β-E2), β-estradiol-3-β-D-glucuronide (β-E2G), propofol (PRO), testosterone (TST), trifluoperazine (TFP), UDP-glucuronic acid (UDPGA; sodium salt), and zidovudine (AZT) were purchased from Sigma-Aldrich (Sydney, Australia). Codeine 6-O-β-D-glucuronide (C6G) and deferiprone 3-O-β-D-glucuronide (DEFG) were purchased from Toronto Research Chemicals (North York, ON, Canada). Lamotrigine (LTG) and lamotrigine N2-β-D-glucuronide (LTG-G) were a gift from the Wellcome Research Laboratories (Beckenham, UK), and deferiprone (DEF) was kindly supplied by Dr John Connelly (ApoPharma Inc, Toronto, ON, Canada). Niflumic acid (NFA) was a gift from the Squibb Institute for Medical Research (Princeton, NJ, USA). Supersomes expressing UGT2B4, UGT2B7 and UGT2B15 were purchased from BD Biosciences (San Jose, CA, USA). Solvents and other reagents used were of analytical reagent grade.

Methods

Human liver microsomes and recombinant UGTs

Human liver microsomes (HLM) were prepared from the hepatic tissue of five donors (HL7, HL10, HL12, HL13 and HL40) by differential ultracentrifugation according to Bowalgaha et al. (2005) and, where indicated, pooled by mixing equal protein amounts. Livers were obtained from the tissue ‘bank’ of the Department of Clinical Pharmacology, Flinders Medical Centre. Approval for the use of human liver tissue for in vitro drug metabolism studies was obtained from the Flinders Clinical Research

DMD Fast Forward. Published on January 18, 2011 as DOI: 10.1124/dmd.110.037036
This article has not been copyedited and formatted. The final version may differ from this version.

Ethics Committee. HLM were activated by pre-incubation with the pore-forming agent alamethicin (50 μg/mg microsomal protein) prior to use in incubations, as described by Boase and Miners (2002).

Human UGT 1A1, 1A3, 1A4, 1A6, 1A7, 1A8, 1A9, 1A10, and 2B17 cDNAs were stably expressed in a human embryonic kidney cell line (HEK293T) (Uchaipichat *et al*., 2004). After growth to at least 80% confluence, cells were harvested and washed in phosphate-buffered saline. Cells were subsequently lysed by sonication using a Vibra Cell VCX 130 Ultrasonics Processor (Sonics and Materials, Newtown, CT, USA). Lysates were centrifuged at 12,000 g for 1 min at 4°C, and the supernatant fraction was separated and stored in phosphate buffer (0.1 M, pH 7.4) at -80°C until use. Given the relatively higher expression of UGT 2B4, 2B7 and 2B15 in Sf cells, Supersomes expressing these proteins were used for activity and inhibition studies. Expression of all UGT proteins was demonstrated by immunoblotting with a commercial UGT1A antibody (BD Gentest, Woburn, MA, USA) or a non-selective UGT antibody (raised against purified mouse Ugt) (Uchaipichat et al., 2004), and by activity measurement (see below).

NFA inhibition of recombinant UGT enzyme activities

NFA was screened for inhibition of UGT 1A1, 1A3, 1A6, 1A7, 1A8, 1A9, 1A10, 2B7, 2B15 and 2B17 activities using the non-selective UGT substrate 4MU as the probe. Incubations were performed at a 4MU concentration corresponding to the apparent K_m or S_{50} of each enzyme (Uchaipichat et al., 2004), in the absence and presence of NFA (1, 10 and 100 μM). NFA stock solutions were prepared in DMSO such that the final concentration of solvent in incubations was 1% (v/v), which has a

DMD Fast Forward. Published on January 18, 2011 as DOI: 10.1124/dmd.110.037036
This article has not been copyedited and formatted. The final version may differ from this version.

negligible or minor effect on most UGT activities (Uchaipichat et al., 2004). An equivalent volume of DMSO was included in control incubations. Protein concentrations and incubation time varied for each enzyme, and were as described by Uchaipichat et al. (2004). Incubations, in a total volume of 200 µl, contained, $MgCl_2$ (4 mM), UDPGA (5 mM), HEK293T cell lysate or Supersomes, and 4MU in phosphate buffer (0.1 M, pH 7.4). Reaction mixtures were pre-incubated at 37°C for 5 min prior to initiation of the reaction by addition of cofactor (UDPGA). Incubations were performed in air at 37°C (shaking water bath) for the specified time for each enzyme (Uchaipichat et al., 2004), and then terminated by the addition of 70% of perchloric acid (2 µl). Mixtures were vortex mixed and centrifuged at 4000 x g for 10 min. Formation of 4MUG was quantified by HPLC following the procedure described by Lewis et al. (2007).

Inhibition of UGT1A4 by NFA was assessed with LTG as the probe substrate according to Rowland et al. (2006). Incubations, in a total volume of 200 µl, contained, $MgCl_2$ (4 mM), UDPGA (5 mM), HEK293 cell lysate expressing UGT1A4 (1 mg/ml), LTG (1500 µM) and NFA (0, 10 and 100 uM). LTG 2-glucuronide was measured by HPLC (Rowland et al., 2006). Effects of NFA on UGT2B4 activity were determined with COD as the substrate (Raungrut et al., 2010). In brief, incubations in a total volume of 100 µl, contained, $MgCl_2$ (4 mM), UDPGA (5 mM), Supersomes expressing UGT2B4 (1 mg/ml), COD (2000 µM), and NFA (0, 1, 10 and 100 µM). Incubations were performed at 37˚C for 120 min. C6G formation was quantified by HPLC (Raungrut et al., 2010).

DMD Fast Forward. Published on January 18, 2011 as DOI: 10.1124/dmd.110.037036
This article has not been copyedited and formatted. The final version may differ from this version.

NFA inhibition of human liver microsomal UGT 1A1, 1A4, 1A6, 1A9, 2B7, 2B15/17 activities.

NFA was screened for inhibition of human liver microsomal UGT 1A1, 1A4, 1A6, 1A9, 2B7, 2B15/17 activities using β-E2, TFP, DEF, PRO, AZT and TST as the respective probe substrates (Miners et al., 2010a). Inhibition, relative to control activities, was characterized for three NFA concentrations (1, 10 and 100 μM; see above) at probe substrate concentrations corresponding to the approximate K_m or S_{50} for each compound with HLM as the enzyme source; β-E2, 40 μM (Soars et al., 2003); TFP, 60 μM (Uchaipichat et al., 2006a); DFP, 4000 μM (Bowalgaha and Miners, unpublished data); PRO, 125 μM (Rowland et al., 2008); AZT, 1000 μM (Boase and Miners, 2002); and TST, 5 μM (Bowalgaha et al., 2007). Studies were performed with pooled HLM from 5 livers (HL 7, 10, 12, 13, and 40). Microsomal protein concentrations, incubation times and HPLC conditions for the TFP, PRO, AZT and TST glucuronidation assays were as described by Uchaipichat et al. (2006a), Rowland et al. (2008), Boase and Miners (2002), and Bowalgaha et al. (2007), respectively.

For experiments investigating inhibition of β-E2 3-glucuronidation with pooled HLM as the enzyme source, incubations contained pooled HLM protein (0.2 mg/ml), phosphate buffer (0.1 M, pH 7.4), $MgCl_2$ (4 mM), UDPGA (5 mM), β-E2, with and without NFA, in a total volume of 200 μl. Incubations were carried out for 30 min at 37˚C and β-E2G formation was quantified by HPLC according to Udomuksorn et al. (2007).

DMD Fast Forward. Published on January 18, 2011 as DOI: 10.1124/dmd.110.037036
This article has not been copyedited and formatted. The final version may differ from this version.

Incubations characterizing human liver microsomal DEF 3-glucuronidation activity contained DEF (4,000 µM), HLM protein (0.5 mg/ml), $MgCl_2$ (4 mM) and UDPGA (5 mM) in phosphate buffer (200 µl; 0.1 M, pH 7.4). Reactions were performed for 60 min and 37ºC, after which time samples were treated with 70% $HClO_4$ (2 µl). Following centrifugation (4,000 x g for 10 min), a 15 µl aliquot of the supernatant fraction was injected on to the HPLC column. HPLC was performed using 1100 series instrument (Agilent Technologies, Sydney, Australia) fitted with a Waters Novapak C18 analytical column (3.9 x 150 mm, 5 µm particle size; Waters, Milford, MA). Analytes were detected by UV absorbtion at 280 nm. The mobile phase comprised of 5mM heptanesulfonic acid in water (pH 2.2) (A) and acetonitrile (B), delivered at a flow rate of 1 ml/min. Initial conditions were 98% A – 2% B increasing linearly to 83% A – 17% B over 10 min, which was held constant for 1.5 min before returning to the initial conditions. DEFG and DEF eluted at 4.9 and 8.8 min, respectively. DEFG was quantified by reference to a standard curve constructed using the authentic compound. Overall within-day assay reproducibility was assessed by measuring DEFG formation at low (0.5 mM) and high (10 mM) substrate concentrations on nine occasions with pooled HLM as the enzyme source. Within-day coefficients of variation were 3.5% and 1.6% at 0.5 and 10 mM, respectively.

Kinetic characterization of NFA inhibition of UGT1A1, UGT1A9, and UGT2B15

Mechanisms of inhibition and inhibitor constants for NFA inhibition of UGT1A1 and UGT1A9 were determined with the individual recombinant enzymes and with pooled HLM, while inhibition of UGT2B15 was characterized only with the recombinant enzyme (due to the lack of convenient selective probes suitable for measurement of microsomal enzyme activity). Incubation conditions were as described in previous

sections, unless specified otherwise. Control activities were determined in the absence of NFA in all experiments.

UGT1A1. Studies with recombinant UGT1A1 were conducted with 4MU and β-E2 as the probe substrates, while experiments with HLM as the enzyme source used only β-E2. Experiments to determine the inhibitor constants with UGT1A1 as the enzyme source included four NFA concentrations (5, 10, 15 and 20 μM) at each of three β-E2 (7.5, 15, and 40 μM) and 4MU (30, 60 and 120 μM) concentrations. Similarly, studies with pooled HLM employed four concentrations of NFA (5, 10, 20 and 50 μM) at each of three concentrations of β-EST (15, 30 and 60 μM).

UGT1A9. Experiments to characterize NFA inhibition of UGT1A9 were as described for UGT1A1, except that PRO was used as the UGT1A9 selective substrate with HLM as the enzyme source. Four NFA concentrations (0.2, 0.4, 0.6 and 0.8 μM) at each of three 4MU (5, 10 and 15 μM) and PRO (20, 40 and 100 μM) concentrations were employed to determine the inhibitor constants with UGT1A9 as the enzyme source. Inhibition experiments with pooled HLM similarly employed four NFA concentrations (0.25, 0.5, 1 and 1.5μM) at each of PRO three concentrations (60, 100 and 200 μM).

UGT2B15. NFA inhibition of UGT2B15 glucuronidation was investigated using Supersomes expressing UGT2B15 as the enzyme source and 4MU as the substrate. Incubation and assay conditions were as described under UGT1A1. The Supersome protein concentration and incubation time were 0.25 mg/ml and 90 min, respectively. Experiments to determine inhibitor constants included four NFA concentrations (20, 40, 60 and 80 μM) at each of three 4MU concentrations; 50, 150 and 300μM.

DMD Fast Forward. Published on January 18, 2011 as DOI: 10.1124/dmd.110.037036
This article has not been copyedited and formatted. The final version may differ from this version.

APAP glucuronidation assay and NFA inhibition of APAP glucuronide formation

APAP glucuronidation kinetic studies were performed with microsomes from three separate human livers (H12, H13, and H40) and the individual recombinant UGTs shown to glucuronidate this compound in activity screening experiments. Linearity of product formation with respect to incubation time and protein concentration for HLM and expressed UGT enzymes was confirmed prior to kinetic studies. Incubations, in a total volume of 200 µl contained, phosphate buffer (0.1 M, pH 7.4), $MgCl_2$ (4 mM), UDPGA (5 mM), HLM (1mg/ml), and APAP (12 concentrations in the range 0.05 - 40 mM). Reactions were performed for 80 min at 37°C (shaking water bath), terminated by the addition of 70% $HClO_4$ (2µl) and then vortex mixed and centrifuged (4000 x g for 10 min). An identical procedure was employed for kinetic studies with recombinant UGTs, except the incubation time was increased to 120 min. A 100 µl aliquot of the supernatant fraction was mixed with 15 µl of 1M sodium acetate to increase the pH of samples prior to analysis by HPLC. HPLC was performed using 1100 series instrument (Agilent Technologies) fitted with a Synergie Hydro reverse-phase C18 analytical column (3 x 150 mm, 4 µm particle size) (Phenomenex, Sydney, Australia). The mobile phase comprised glacial acetic acid - acetonitrile – water (1:5:94). Analytes were eluted at a flow rate of 1 ml/min and detected by UV absorption at 243 nm. Under these conditions, retention times for APAPG and APAP were 1.7 and 3.5 min, respectively. APAPG concentrations in incubation mixtures were quantified by comparison of peak areas to those of an APAPG standard curve. Within-day overall assay reproducibility for the APAP glucuronidation assay was assessed by measuring the rate of APAPG formation in

nine separate incubations of pooled HLM; coefficients of variations were 5.2% and 3.0% for APAP concentrations of 0.25mM and 10mM, respectively.

The kinetics of human liver microsomal APAP glucuronidation across the substrate concentration range employed in kinetic studies (12 concentrations in the range 0.05 - 40 mM) were further characterized in the absence and presence of 3 NFA concentrations (2.5, 50 and 100μM). Inhibition experiments were conducted with microsomes from the same three livers used in the kinetic studies (viz. HL12, H13 and H40). NFA inhibition of APAP glucuronidation by recombinant UGT1A1, UGT1A6, UGT1A9, and UGT2B15 was determined at four NFA concentrations (2.5, 5, 50 and 100μM) at APAP concentrations corresponding to the K_m or S_{50} for each enzyme (see Results).

Data Analysis

All kinetic and inhibition experiments were performed in duplicate and data points represent the mean of duplicate estimates (<10% variance). APAP glucuronidation kinetic data were modeled using the Michaelis Menten equations for single and two-enzyme reactions, the Hill equation and the substrate inhibition equation (see Uchaipichat et al., 2004 for expressions) using EnzFitter version 2.0 (Biosoft, Cambridge, UK). Similarly, the mechanism of inhibition and K_i values for NFA inhibition of UGT activities were determined by fitting the expressions for competitive, noncompetitive, uncompetitive and mixed inhibition to experimental data using Enzfitter. (Given the importance of mechanism of inhibition to the Results and their interpretation, equations corresponding to each mechanism are given below.) Goodness of fit of all expressions was assessed from comparison of the parameter SE of fit, coefficient of determination (r^2), 95% confidence intervals, and F-statistic.

DMD Fast Forward. Published on January 18, 2011 as DOI: 10.1124/dmd.110.037036
This article has not been copyedited and formatted. The final version may differ from this version.

Competitive inhibition:

$$v = \frac{V_{max} \times [S]}{K_m(1+[I]/K_i)+[S]}$$

where V_{max} is maximal velocity, [S] is substrate concentration, K_m is the Michaelis constant, and K_i is the inhibitor constant (for the EI complex).

Non-competitive inhibition:

$$v = \frac{V_{max} \times [S]}{(1+[I]/K_i)(K_m+[S])}$$

where K_i is the inhibitor constant for the EI and ESI complexes.

Mixed (competitive – non-competitive) inhibition:

$$v = \frac{V_{max} \times [S]}{K_m(1+[I]/K_i)+[S](1+[I]/K_i')}$$

where K_i and K_i' are the inhibitor constants for the EI and ESI complexes, respectively. K_i' is related to K_i by a factor, α (> 1), that is EI has a lower affinity for the substrate than does E (Segel 1993).

RESULTS

NFA inhibition of recombinant and human liver microsomal UGT enzyme activities

The selectivity of NFA as an inhibitor of human UGTs was characterized initially with recombinant proteins. 4MU was used as the probe substrate for the inhibition studies with UGT 1A1, 1A3, 1A6, 1A7, 1A8, 1A9, 1A10, 2B7, 2B15 and 2B17. Since UGT1A4 and UGT2B4 exhibit low or negligible activity towards 4MU (Uchaipichat et al., 2004; Kubota et al., 2007), LTG and COD were used as the respective substrates (Raungrut et al., 2010; Rowland et al., 2006). NFA was a potent inhibitor of UGT1A7 and UGT1A9. The activity of both enzymes was abolished by 10μM NFA (Figure 1). UGT1A1, UGT1A6, UGT1A8, UGT1A10, UGT2B15 and UGT2B17 activities were inhibited by approximately 30% – 90% at an added NFA concentration of 100μM, whereas UGT1A3, UGT1A4, UGT2B4 and UGT2B7 were inhibited by ≤ 25%. While inhibition of UGT1A7, UGT1A8 and UGT1A10 is notable, especially the potent effect of NFA on UGT1A7, inhibition of these enzymes was not studied further since expression in liver and kidney is minor or negligible (Ohno and Nakajin, 2009).

The results of inhibition screening studies of human liver microsomal UGT activities were broadly consistent with the recombinant enzyme data. PRO glucuronidation, a selective marker of hepatic UGT1A9 activity, was inhibited by 72% and 95% at NFA concentrations of 1 and 10 μM, respectively (Figure 2). NFA, 100 μM, caused 36% to 81% inhibition of β-E2 (UGT1A1), DEF (UGT1A6), and TST (UGT2B15/17) glucuronidation, but minimal inhibition of TFP (UGT1A4) and AZT (UGT2B7) glucuronidation (Figure 2). The inhibition of human liver microsomal PRO glucuronidation across the NFA concentration range investigated was somewhat lower than the inhibition observed with 4MU glucuronidation by recombinant

DMD Fast Forward. Published on January 18, 2011 as DOI: 10.1124/dmd.110.037036
This article has not been copyedited and formatted. The final version may differ from this version.

UGT1A9. This is not unexpected since long-chain unsaturated fatty acids released from the microsomal membrane during the course of an incubation contribute significantly to the inhibition observed with HLM as the enzyme source (Rowland et al., 2008).

Kinetic characterization of NFA inhibition of recombinant and human liver microsomal UGT activities

Kinetic studies to determine values of the inhibitor constant were performed with those recombinant UGTs and human liver microsomal UGT activities exhibiting IC_{50} values < 200 μM in the inhibition screening studies (i.e. UGT1A1, UGT1A9 and UGT2B15; Figures 1 and 2). Inhibition experiments with recombinant UGT 1A1, 1A9 and 2B15 all employed 4MU as the substrate. Additionally, β-E2 and PRO were utilized as selective substrate probes for the kinetic characterization of NFA inhibition of recombinant and human liver microsomal UGT1A1 and UGT1A9, respectively. Notably, NFA was a potent inhibitor of the glucuronidation of 4MU and PRO by UGT1A9, and human liver microsomal PRO glucuronidation. In all cases, data were best described by the expression for mixed (competitive – non-competitive) inhibition (Figure 3). Derived K_i values were in the range 0.10 to 0.40 μM (Table 1). As indicated above, higher K_i values are expected with HLM as the enzyme source due to the added inhibitory effects of membrane long-chain unsaturated fatty acids. Derived K_i' (dissociation constant for the ESI complex) values were 3- to 7- fold higher than the corresponding K_i's.

Like the inhibition pattern observed for UGT1A9, NFA was a mixed (competitive – non-competitive) inhibitor of human liver microsomal and UGT1A1 catalyzed β-E2

DMD Fast Forward. Published on January 18, 2011 as DOI: 10.1124/dmd.110.037036
This article has not been copyedited and formatted. The final version may differ from this version.

glucuronidation (Figure 4), although the similar K_i and K_i' values obtained for NFA inhibition of the UGT1A1 catalyzed reaction (Table 1) are consistent with only a marginally better fit with the equation for mixed (compared to non-competitive) inhibition. The effect of NFA on 4MU glucuronidation by UGT1A1 was best modeled using the equation for non-competitive inhibition (Figure 4A). The derived K_i values for NFA inhibition of UGT1A1 catalyzed 4MU and β-E2 glucuronidation (viz. 14 to 18 μM) were approximately 2-orders of magnitude higher than those observed for UGT1A9 (Table 1). Given the lack of a convenient selective substrate probe for UGT2B15 suitable for studies with HLM, NFA inhibition of this enzyme was assessed with the recombinant protein and 4MU as substrate. Interestingly, NFA inhibition of UGT2B15 was competitive (Figure 5 and Table 1), compared to the mixed or non-competitive inhibition observed with the other enzymes investigated here.

APAP glucuronidation and inhibition by NFA

The 14 recombinant UGT enzymes investigated here were screened for the ability to glucuronidate APAP (0.5, 5 and 50 mM). Activities were determined using a HEK293 lysate/Supersome protein concentration of 1 mg/ml and an incubation time of 120 min. UGT1A1, UGT1A6, UGT1A9 and UGT2B15 were the only hepatically expressed enzymes that glucuronidated APAP (data not shown). APAP glucuronidation by UGT1A1 and UGT1A9 exhibited sigmoidal kinetics, which was modeled using the Hill equation (Figure 6). In contrast, the Michaelis-Menten and substrate inhibition equations provided the best fit for APAP glucuronidation by UGT1A1 and UGT2B15, respectively, although deviation from substrate inhibition kinetics was observed for UGT2B15 catalyzed APAPG formation at low substrate

DMD Fast Forward. Published on January 18, 2011 as DOI: 10.1124/dmd.110.037036
This article has not been copyedited and formatted. The final version may differ from this version.

concentrations. Derived kinetic parameters are given in Table 2. NFA inhibition of APAP glucuronidation by recombinant UGT1A1, UGT1A6, UGT1A9, and UGT2B15 was determined at four NFA concentrations (2.5, 5, 50 and 100μM) at the APAP concentration corresponding to the K_m or S_{50} for each of these enzymes. Consistent with the inhibition data shown in Figures 1, 2 and 3, NFA 5 μM essentially abolished APAP glucuronidation by UGT1A9 (Figure 7).

APAP glucuronidation kinetics were characterized in the presence of increasing concentrations of NFA (0, 2.5, 50 and 100 μM) using microsomes from 3 livers (HL 12, 13, 40) (Figure 8 and Table 3). Although there was a suggestion of deviation from hyperbolic kinetics at low substrate concentrations (Figure 8), as has been observed by other investigators (Court et al., 2001; Mutlib et al., 2006), the single enzyme Michaelis-Menten equation provided the best fit to experimental data (on the basis of of goodness-of-fit parameters; see Data Analysis). Mean V_{max} values for human liver microsomal APAP glucuronidation decreased (relative to control) by 20%, 35% and 40% with increasing NFA concentrations between 2.5 and 100 μM. K_m values also tended to decrease with increasing NFA concentration, with a 26% decrement in mean K_m between 0 and 100 μM NFA (17 μM vs. 12.6 μM).

DISCUSSION

Enzyme selective inhibitors arguably represent the most valuable experimental tool for the reaction phenotyping of drug and xenobiotic metabolism reactions in vitro. The extent of inhibition of the glucuronidation, or indeed any other pathway (e.g. oxidative metabolism by cytochromes P450), of a test compound by HLM or hepatocytes by an enzyme selective inhibitor under appropriate experimental conditions reflects the contribution of that UGT enzyme to in vitro intrinsic clearance (Miners et al., 2010a). The present study has demonstrated that a low concentration (2.5 μM) of NFA selectively inhibits UGT1A9, while inhibition by 50 μM NFA primarily provides a measure of the combined contributions of UGT1A9 and UGT1A1 to a glucuronidation reaction (see following discussion).

Although NFA appears to be metabolized by UGT1A1 (Mano et al., 2006a), NFA was shown here to be a potent inhibitor of UGT1A9. K_i values ranged from 0.10 to 0.40 μM depending on the substrate and enzyme source (recombinant enzyme or HLM). It should be noted that the inhibitor constants derived for NFA inhibition of PRO glucuronidation by HLM may be overestimated by as much as an order of magnitude due to the combined inhibitory effects of long-chain unsaturated fatty acids released from the microsomal membrane during the course of an incubation (Rowland et al., 2007 and 2008). K_i values generated using recombinant UGT1A9 are also likely to be over-estimated, but to a lesser extent (Rowland et al., 2008). Although the 'true' K_i values may be estimated from experiments performed in the presence of BSA, which sequesters the inhibitory fatty acids, NFA binds extensively to albumin thereby precluding the addition of BSA to incubations. The K_i for NFA inhibition of 4MU glucuronidation by recombinant UGT1A9 found here is in reasonable agreement with

the value (0.03 μM) reported by Mano et al. (2006b), although the previous study assumed competitive inhibition.

Substantially lesser inhibition was observed with UGT enzymes other than UGT1A9. K_i values for NFA inhibition of human liver microsomal UGT1A1 and UGT2B15 were 15 μM and 62 μM, respectively. Based on data given in Figures 1 and 2, IC_{50} values for NFA inhibition of UGT1A3, UGT1A4, UGT1A6, UGT2B4, UGT2B7 and UGT2B17 exceed 200 μM. Substituting the K_i values obtained here for UGT1A1, UGT1A9 and UGT2B15 in the expression for the reduction in enzyme activity at a given inhibitor concentration [I] (i.e. $v_i/v = 1/\{1 + [I]/K_i\}$) predicts that 2.5 μM NFA inhibits UGT1A9 and UGT1A1 by 86% and 14%, respectively, with negligible effects on UGT2B15. At a concentration of 50 μM, NFA is predicted to inhibit UGT1A9, UGT1A1 and UGT2B15 by 95%, 77% and 45%, respectively, while at 100 μM predicted inhibition of UGT1A9, UGT1A1 and UGT2B15 is 99%, 87% and 62%, respectively.

Apart from UGT2B15, which was competitively inhibited by NFA, the mechanism of inhibition of the UGTs characterized here was non-competitive or mixed (competitive – non-competitive). The usual model of non-competitive inhibition assumes that: the substrate and inhibitor bind randomly, reversibly and independently at two distinct sites; the ESI complex is non-productive; and the dissociation constant of each compound is unaffected by the binding of the other (Segel 1993). Mixed competitive – non-competitive inhibition requires the dissociation constant for the ESI complex to be higher than that for EI. Importantly, V_{max} is reduced by both mechanisms but binding affinity is decreased only for mixed inhibition. The notion of multiple

substrate and modifier binding sites is consistent with the results of recent kinetic studies with recombinant and human liver microsomal UGTs (Stone et al., 2003; Uchaipichat et al., 2004 and 2008; Williams et al., 2002; Zhou et al., 2010). The different mechanisms of UGT1A1 inhibition with β-E2 and 4MU as the substrates may reflect differing binding orientations of these compounds within the UGT1A1 active site or potential contribution of UGT1A3 to the human liver microsomal reaction (Lepine et al., 2004; Miners et al., 2010a). However, K_i values for NFA inhibition were comparable with both substrates. Similarly, K_i values for NFA inhibition of UGT1A9 were close in value with both 4MU and PRO as the substrates. As noted previously, the higher K_i observed for human liver microsomal UGT1A9 probably reflects the greater inhibitory effect of long-chain unsaturated fatty acids with this enzyme source (Rowland et al., 2007 and 2008).

Despite APAP being one of the most widely used drugs worldwide the relative contribution of individual UGT enzymes to APAP glucuronidation is yet to be completely resolved. Initial studies with recombinant UGT enzymes demonstrated that UGT1A1, UGT1A6 and UGT1A9 exhibit highest activity towards APAP (Bock et al., 1993; Court et al., 2001). However, more recently UGT2B15 has also been shown recently to catalyze APAP glucuronidation (Mutlib et al., 2006). Consistent with these reports, UGT1A1, UGT1A6, UGT1A9 and UGT2B15 were all shown here to glucuronidate APAP (Figure 6), and APAP glucuronidation kinetic models differed between enzymes. Like these authors we found APAP glucuronidation by UGT1A1 and UGT2B15 followed sigmoidal and substrate inhibition kinetics, respectively. Similarly, our data for UGT1A9 are in agreement with the sigmoidal kinetics reported by Court et al. (2001). While Mutlib et al. (2006) assumed hyperbolic kinetics for

UGT1A9, the Eadie-Hofstee plot shown in their report strongly suggests atypical (sigmoidal) kinetics. In contrast to both Court et al. (2001) and Mutlib et al. (2006) who reported substrate inhibition kinetics for APAP glucuronidation by UGT1A6, we observed hyperbolic kinetics (Figure 6). The reasons for discrepancies between studies are not clear, but may arise from differences in: expression systems (HEK293 cells here for UGT1A enzymes versus Supersomes in the other studies) and the relative expression of recombinant UGTs; kinetic modelling approaches; substrate concentration ranges employed in kinetic studies; and the interpretation of glucuronidation kinetic data (Miners et al., 2010a). While it is noteworthy that K_m/S_{50} values determined here for APAP glucuronidation by UGT1A1, UGT1A6 and UGT1A9 are in very close agreement with those reported by Court et al. (2001), the rank order of V_{max} values differed.

Based on correlations between the rates of APAP, bilirubin (UGT1A1) and propofol (UGT1A9) glucuronidation, and immunoreactive UGT1A6 activity in a panel of HLM along with the kinetic parameters for APAP glucuronidation by recombinant UGT1A1, UGT1A6 and UGT1A9, Court et al. (2001) predicted that UGT1A9 accounted for approximately 60% of APAP glucuronidation in humans. This model further predicted that the relative contributions of UGT1A1 and UGT1A6 to APAP glucuronidation increased and decreased, respectively, with increasing substrate concentration. It should be noted, however, that comparisons of UGT activities between enzyme sources may be problematic. In particular, differences can occur in the kinetic mechanism and derived constants for the same reaction catalyzed by different enzyme sources (e.g. HLM and a recombinant UGT; see for example Bowalgaha et al., 2005) and for the same recombinant UGT enzyme expressed in

different laboratories (e.g. Itaaho et al., 2008). The former point is further exemplified here; APAP glucuronidation by HLM exhibits hyperbolic kinetics, while atypical kinetics were observed with UGT1A1, UGT1A9 and UGT2B15.

The effects of increasing concentrations of NFA on UGT1A9, UGT1A1 and UGT2B15 activities provides an alternative approach to assessing the relative contributions of each of these enzymes and UGT1A6 to APAP glucuronidation by HLM. NFA, 2.5 μM, which essentially abolishes UGT1A9 activity (including UGT1A9 catalyzed APAP glucuronidation; Figure 7), reduced the V_{max} for human liver microsomal APAP glucuronidation by 20%. The V_{max} was reduced by 35% and 40% in the presence of NFA 50 μM and 100 μM, respectively, concentrations that result in major inhibition of UGT1A1 and UGT2B15. K_m values similarly tended to decrease in parallel with V_{max} as the NFA concentration was increased. Given UGT1A1, UGT1A6, UGT1A9 and UGT2B15 are the only enzymes that contribute to hepatic APAP glucuronidation, the NFA inhibition data suggest that UGT1A6 is the major contributor to APAP glucuronidation across a wide substrate concentration range (Figure 8B), with smaller contributions from UGT1A1, UGT1A9 and UGT2B15.

In summary, it has been demonstrated that NFA at low concentration (2.5 μM) selectively inhibits human liver microsomal UGT1A9. Higher concentrations (50 – 100 μM) further differentiate UGT1A1 and UGT2B15. Along with hecogenin and fluconazole, which are respective selective inhibitors of UGT1A4 and UGT2B7 (Miners et al., 2010a), the availability of NFA as an inhibitor ‘probe’ for UGT1A9 provides a valuable experimental resource for the reaction phenotyping of human liver

microsomal drug glucuronidation. By way of example, the comparative effects of increasing NFA concentrations on APAPG formation by HLM and recombinant UGT enzymes suggest that UGT1A6 is the main enzyme involved in the hepatic glucuronidation of APAP.

ACKNOWLEDGEMENTS

Grant funding from the National Health and Medical Research Council of Australia is gratefully acknowledged.

AUTHORSHIP CONTRIBUTIONS

Participated in research design: Miners, Knights and Baranczewski

Conducted experiments: Bowalgaha and Elliot

Performed data analysis: Miners and Bowalgaha

Wrote or contributed to the writing of the paper: Miners, Knights, Bowalgaha and Baranczewski

Other: Miners and Knights acquired funding for the research

REFERENCES

Bichlmaier I, Kurkela M, Joshi T, Siiskonen A, Ruffer T, Lang H, Suchanova B, Vahermo M, Finel M, Yli-Kauhaluoma J (2007) Isoform-selective inhibition of the human UDP-glucuronosyltransfearse 2B7 by isolongifolol derivatives. *J Med Chem* **50:**2655-2644.

Boase S, Miners JO (2002) In vitro – in vivo correlations for drugs eliminated by glucuronidation: Investigations with the model substrate zidovudine. *Br J Clin Pharmacol* **54:**493-503.

Bock KW, Forster A, Gschaidmeier H, Bruck M, Munzel P, Schareck W, Fournel-Gigleux S and Burchell B (1993) Paracetamol glucuronidation by recombinant rat and human phenol UDP-glucuronosyltransferases. *Biochem Pharmacol* **45:**1809-1814.

Bowalgaha K, Elliot DJ, Mackenzie PI, Knights KM, Swedmark S, Miners JO (2005) Naproxen and desmethylnaproxen glucuronidation by human liver microsomes and recombinant human UDP-glucuronosyltransferases (UGT): Role of UGT2B7 in the elimination of naproxen. *Br J Clin Pharmacol* **60:**423-433.

Bowalgaha K, Elliot DJ, Mackenzie PI, Knights KM and Miners JO (2007) The glucuronidation of Δ4-3-keto C19- and C21- hydroxysteroids by human liver microsomal and recombinant UDP-glucuronosyltransferases (UGTs): 6α- and 21-hydroxyprogesterone are selective substrates for UGT 2B7. *Drug Metab Disp* **35:**363-370 (2007).

Court MH, Duan SX, Von Moltke LL, Greenblatt DJ, Patten CJ, Miners JO and Mackenzie PI (2001) Interindividual variability in acetaminophen glucuronidation by human liver microsomes: Identification of relevant acetaminophen UDP-glucuronosyltransferase isoforms. *J Pharmacol Exp Ther* **299:**998-1006.

Court MH (2005) Isoform-selective probe substrates for in vitro studies of human UDP-glucuronosyltransferases. *Methods Enzymol* **400:**104-116.

Court MH (2010) Interindividual variability in hepatic drug glucuronidation: studies into the role of age, sex, enzyme inducers, and genetic polymorphism using the human liver bank as a model system. *Drug Metab Rev* **42:**209-224.

Court MH (2010) Interindividual variability in hepatic drug glucuronidation: Studies into the role of sex, age, enzyme inducers, and genetic polymorphism using the human liver bank as a model system. *Drug Metab Rev* **42:**209-224.

Gaganis P, Miners JO and Knights KM (2007) Glucuronidation of fenamates: Kinetic studies using human kidney cortical microsomes and recombinant UDP-glucuronosyltransferase (UGT) 1A9 and 2B7. *Biochem Pharmacol* **73:**1683-1691.

Guillemette C (2003) Pharmacogenomics of human UDP-glucuronosyltransferase enzymes. *Pharmacogenomics J* **3:**136-158.

Itaaho K, Mackenzie PI, Ikushiro S, Miners JO and Finel M (2008) The configuration of the 17-hydroxy group variably influences the glucuronidation of β-estradiol and epiestradiol by human UDP-glucuronosyltransferases. *Drug Metab Disp* **36:**2307-2315.

Kiang TKL, Ensom MHH and Chang TKH (2005) UDP-Glucuronosyltransferases and clinical drug-drug interactions. *Pharmacol Ther* **106:**97-132.

Kubota T, Lewis BC, Elliot DJ, Mackenzie PI and Miners JO (2007) Critical roles of residues 36 and 40 in the phenol and tertiary amine aglycone substrate selectivities of UDP-glucuronosyltransferases 1A3 and 1A4. *Molec Pharmacol* **72:**1054-1062.

Lepine J, Bernard O, Plante M, Tetu B, Pelletier G, Labrie F, Belanger A and Guillemette C (2004) Specificity and regioselectivity of the conjugation of estradiol, estrone, and their catcholestrogen and methoxyestrogen metabolites by human uridine diphospho-glucuronosyll transferases expressed in endometrium. *J Clin Endocrinol Metab* **89:**5222-5232.

Lewis BC, Mackenzie PI, Elliot DJ, Burchell B, Bhasker CR and Miners JO (2007) Amino terminal domains of human UDP-glucuronosyltransferases (UGT) 2B7 and 2B15 associated with substrate selectivity and autoactivation. *Biochem Pharmacol* **73:**1463-1473.

Mackenzie PI, Bock KW, Burchell B, Guillemette C, Ikushiro S, Iyanagi T, Miners JO, Owens IS and Nebert DW (2005) Nomenclature update for the mammalian UDP glycosyltransfearse (UGT) gene family *Pharmacogenet Genomics* **15:**677-685.

Mano Y, Usui T and Kamimura H (2006a) Identification of human UDP-glucuronosyltransferase responsible for the glucuronidation of niflumic acid in human liver. *Pharm Res* **23:**1502-1508.

Mano Y, Usui T and Kamimura H (2006b) In vitro inhibitory effects of non-steroidal anti-inflammatory drugs on 4-methylumbelliferone glucuronidation in recombinant human UDP-glucuronosyltransferase 1A9 – Potent inhibition by niflumic acid. *Biopharm Drug Disp* **27:**1-6.

Miners JO, Attwood J, and Birkett DJ (1984) Determinants of acetaminophen metabolism: Effect of inducers and inhibitors of drug metabolism on acetaminophen's metabolic pathways. *Clin Pharmacol Ther* **35:**480-486.

Miners JO and Mackenzie (1991) Drug glucuronidation in humans. *Pharmacol Ther* **51:**347-369.

Miners JO, McKinnon RA and Mackenzie PI (2002) Genetic polymorphisms of UDP-glucuronosyltransferases and their functional significance. *Toxicology* **181-182:**453-456.

Miners JO, Smith PA, Sorich MJ, McKinnon RA and Mackenzie PI (2004) Predicting drug glucuronidation parameters: Application of in vitro and in silico modelling approaches. *Annu Rev Pharmacol Toxicol* **44:**1-25.

Miners JO, Knights, KM, Houston JB and Mackenzie PI (2006) In vitro – in vivo correlation for drugs and other compounds eliminated by glucuronidation in humans: Pitfalls and promises. *Biochem Pharmacol* **71:**1531-1539.

Miners JO, Mackenzie PI and Knights KM (2010a) The prediction of drug glucuronidation parameters in humans: UDP-glucuronosyltransferase enzyme selective substrate and inhibitor probes for reaction phenotyping and in vitro – in vivo extrapolation of drug clearance and drug-drug interaction potential. *Drug Metab Rev* **42:**189-201.

Miners JO, Polasek TM, Mackenzie PI and Knights KM (2010b) The in vitro characterization of inhibitory drug-drug interactions involving UDP-glucuronosyltransferase. In, Enzyme and Transporter based drug-drug interactions (Eds Pang KS, Rodrigues AD and Peter R), Chapter 8, pp 217-236, Springer (New York).

Mutlib AE, Goosen TC, Bauman JN, Williams JA, Kulkarni S and Kostrubsky S (2006) Kinetics of acetaminophen glucuronidation by UDP-glucuronosyltransferases 1A1, 1A6, 1A9 and 2B15. Potential implications in acetaminophen-induced hepatotoxicity. *Chem Res Toxicol* **19:**701-709.

Ohno S and Nakajin S (2009) Determination of mRNA expression of human UDP-glucuronosyltransferases and application for localization in various human

tissues by real-time reverse transcriptase polymerase chain reaction. *Drug Metab Disp* **37:**32-40.

Raungrut P, Uchaipichat V, Elliot DJ, Janchawee B, Somogyi AA and Miners JO (2010) In vitro – in vivo extrapolation predicts drug-drug interactions arising from inhibition of codeine glucuronidation by dextropropoxyphene, fluconazole, ketoconazole and methadone in humans. *J Pharmacol Exp Ther* **334:**609-618 (2010).

Rowland A, Elliot DJ, Williams JA, Mackenzie PI, Dickinson RG and Miners JO (2006) In vitro characterization of lamotrigine N2-glucuronidation and lamotrigine-valproic acid interaction. *Drug Metab Disp* **34:**1055-1062.

Rowland A, Gaganis P, Elliot DJ, Mackenzie PI, Knights KM and Miners JO (2007) Binding of inhibitory fatty acids is responsible for the enhancement of UDP-glucuronosyltransferase 2B7 activity by albumin: Implications for in vitro – in vivo extrapolation. *J Pharmacol Exp Ther* **321:**137-147.

Rowland A, Knights KM, Mackenzie PI and Miners JO (2008) The "albumin effect" and drug glucuronidation: Bovine serum albumin and fatty acid-free human serum albumin enhance the glucuronidation of UDP-glucurososyltransferase (UGT) 1A9 but not UGT1A1 and UGT1A6 activities. *Drug Metab Disp* **36:**1056-1062.

Segel IH (1993) Enzyme Kinetics: Behavior and analysis of rapid equilibrium and Steady-State Enzyme Systems, pp 125-129 and 170-173, J Wiley and Sons, New York.

Soars MG, Ring BJ and Wrighton SA (2003) The effect of incubation conditions on the enzyme kinetics of UDP-glucuronosyltransferases. *Drug Metab Disp* **31:**762-767.

Stone AN, Mackenzie PI, Galetin A, Houston JB and Miners JO (2003) Isoform selectivity and kinetics of morphine 3- and 6- glucuronidation by human

UDP-glucuronosyltransferases: evidence for atypical glucuronidation kinetics by UGT2B7. *Drug Metab Disp* **31:**1086-1089.

Uchaipichat V, Mackenzie PI, Guo X-H, Gardner-Stephen D, Galetin A, Houston JB and Miners JO (2004) Human UDP-glucuronosyltransferases: Isoform selectivity and kinetics of 4-methylumbelliferone and 1-naphthol glucuronidation, effects of organic solvents, and inhibition by diclofenac and probenecid. *Drug Metab Disp* **32:**413-23.

Uchaipichat V, Mackenzie PI, Elliot DJ and Miners JO (2006a) Selectivity of substrate (trifluoperazine) and inhibitor (amitriptyline, androsterone, canrenoic acid, hecogenin, phenylbutazone, quinidine, quinine, and sulfinpyrazone) probes for human UDP-glucuronosyltransferases. *Drug Metab Disp* **34:**449-456.

Uchaipichat V, Winner LK, Mackenzie PI, Elliot DJ, Williams JA and Miners JO (2006b) Quantitative prediction of in vivo inhibitory interactions involving glucuronidated drugs from in vitro data: The effect of fluconazole on zidovudine glucuronidation. *Br J Clin Pharmacol* **61:**427-439.

Uchaipichat V, Galetin A, Houston JB, Mackenzie PI, Williams JA and Miners JO (2008) Kinetic modeling of the interactions between 4-methylumbelliferone, 1-naphthol and zidovudine glucuronidation by UDP-glucuronosyltransferase 2B7 (UGT2B7) provides evidence for multiple substrate binding and effector sites. *Molec Pharmacol* **74:**1152-1162.

Udomuksorn W, Elliot DJ, Lewis BC, Mackenzie PI, Yoovathaworn K and Miners JO (2007) Influence of mutations associated with Gilbert and Crigler-Najjar type II syndromes on glucuronidation kinetics of bilirubin and other UDP-glucuronosyltransferase 1A substrates. *Pharmacogenet Genomics* **17:**1017-1029.

Vietri M, Pietrabissa A, Mosca F and Pacifici GM (2002) Inhibition of mycophenolic acid glucuronidation by niflumic acid in human liver microsomes. *Eur J Clin Pharmacol* **58:**93-97.

Williams JA, Ring BJ, Cantrell VE, Campanele K, Jones DR, Hall SD, and Wrighton SA (2002) Differential modulation of UDP-glucuronosyltransferase 1A1 (UGT1A1) catalyzed estradiol 3-glucuronidation by the addition of UGT1A1 substrates and other compounds to human liver microsomes. *Drug Metab Disp* **30:** 1266-1273.

Zhou J, Tracy TS and Remmel R (2010) Glucuronidation of dihydrotestosterone and trans-androsterone by recombinant UDP-glucuronosyltransferase (UGT) 1A4: Evidence for multiple aglycone binding sites. *Drug Metab Disp* **38:**431-440.

LEGENDS TO FIGURES

Figure 1. Effects of NFA (0, 1, 10 and 100 μM) on the activities of recombinant human UGT enzymes. 4MU was used as probe the substrate, except for UGT1A4 (LTG) and UGT2B4 (COD). The 4MU, LTG and COD concentrations correspond to the known K_m or S_{50} values for each substrate and enzyme. Each bar represents the mean of duplicate measurements.

Figure 2. Effects of NFA (0, 1, 10 and 100 μM) on the activities of human liver microsomal UGT1A1, 1A4, 1A6, 1A9, 2B7 and 2B15/17 activities determined with β-E2, TFP, DEF, PRO, AZT and TST as the respective probe substrates. Concentrations of each substrate correspond to their published K_m values with HLM as the enzyme source. Experiments were performed with pooled HLM from 5 livers (HL 7, 10, 12, 13, 40), and each bar represents the mean of duplicate measurements.

Figure 3. Dixon plots for NFA inhibition of 4MU glucuronidation by recombinant UGT1A9, and PRO glucuronidation by recombinant UGT1A9 and pooled HLM. Each point represents the mean of duplicate measurements while lines are from model fitting.

Figure 4. Dixon plots for NFA inhibition of 4MU glucuronidation by recombinant UGT1A1, and β-EST glucuronidation by recombinant UGT1A1 and pooled HLM. Each point represents the mean of duplicate measurements while lines are from model fitting.

Figure 5. Dixon plot for NFA inhibition of 4MU glucuronidation by recombinant UGT2B15. Each point represents the mean of duplicate measurements while lines are from model fitting.

Figure 6. Eadie-Hofstee plots for APAP glucuronidation by recombinant UGT1A1, UGT1A6, UGT1A9 and UGT2B15. Each point represents the mean of duplicate measurements while curves are from model fitting.

Figure 7. Effect of NFA (0, 1, 10 and 100 μM) on APAP glucuronidation by recombinant UGT1A1, UGT1A6, UGT1A9, and UGT2B15. APAP concentrations corresponded to the K_m or S_{50} for each enzyme. Each bar represents the mean of duplicate measurements.

Figure 8. Representative velocity versus substrate concentration (A) and Eadie-Hofstee (B) plots for APAP glucuronidation by HLM (HL 40) in the presence of increasing concentrations of NFA (0, 2.5, 50 and 100 μM). Each point represents the mean of duplicate measurements while curves/lines are from model fitting.

DMD Fast Forward. Published on January 18, 2011 as DOI: 10.1124/dmd.110.037036
This article has not been copyedited and formatted. The final version may differ from this version.

Table 1. Derived kinetic parameters for niflumic acid inhibition of recombinant and human liver microsomal UGT1A1, UGT1A9 and UGT2B15 activities[a]

Enzyme Source	Substrate[b]	Mechanism of inhibition	K_i[c] (μM)	K_i'[d] (μM)
UGT1A1	4MU	non-competitive	14 ± 0.1	n/a
UGT1A1	β-E2	mixed	18 ± 1.3	19 ± 1.1
HLM	β-E2	mixed	15 ± 1.2	34 ± 3.0
UGT1A9	4MU	mixed	0.11 ± 0.01	0.30 ± 0.14
UGT1A9	PRO	mixed	0.10 ± 0.002	0.7 ± 0.11
HLM	PRO	mixed	0.40 ± 0.05	1.6 ± 0.12
UGT2B15	4MU	competitive	62 ± 2.6	n/a

[a] Data presented as parameter ± SE of parameter fit

[b] β-EST, β-estradiol; 4MU, 4-methylumbelliferone; DEF, deferiprone; PRO, propofol

[c] K_i is the dissociation constant for the EI and ESI complex in non-competitive and the EI complex in mixed inhibition

[d] K_i' is the dissociation constant for the ESI complex in mixed inhibition

n/a, not applicable

DMD Fast Forward. Published on January 18, 2011 as DOI: 10.1124/dmd.110.037036
This article has not been copyedited and formatted. The final version may differ from this version.

Table 2. Derived kinetic parameters for acetaminophen glucuronidation by recombinant human UGT enzymes[a]

Enzyme	Equation[b]	K_m or S_{50} (mM)	V_{max} (pmol/min mg)	K_{si} (mM)	n
UGT1A1	Hill	8.7 ± 0.3	26 ± 0.4	n/a	1.38 ± 0.04
UGT1A6	MM	2.2 ± 0.05	367 ± 2.6	n/a	n/a
UGT1A9	Hill	25 ± 0.4	1087 ± 12	n/a	1.60 ± 0.02
UGT2B15	SI	7.6 ± 1.0	344 ± 15	36 ± 5.0	n/a

[a]Data presented as parameter ± SE of parameter fit

[b]MM, Michaelis-Menten; SI, substrate inhibition

n/a, not applicable

Table 3. Effect of niflumic acid (2.5, 50 and 100 µM) on the kinetics of APAP glucuronidation by HLM.

Liver number	**Control (no NFA)**		**2.5 µM NFA**		**50 µM NFA**		**100 µM NFA**	
	K_m **(**mM)	**V_{max}** (pmol/min.mg)	**K_m** **(**mM)	**V_{max}** (pmol/min.mg)	**K_m** **(**mM)	**V_{max}** (pmol/min.mg)	**K_m** **(**mM)	**V_{max}** (pmol/min.mg)
HL12	18 ± 0.2	2355 ± 10	13 ± 0.1	1872 ± 7	14 ± 0.3	1702 ± 17	14 ± 0.6	1592 ± 31
HL13	22 ± 0.1	2423 ± 65	17 ± 0.9	1868 ± 50	15 ± 0.1	1290 ± 4	15 ± 0.1	1180 ± 3
HL40	11 ± 0.009	3376 ± 1.0	9.9 ± 0.02	2792 ± 1.8	9.9 ± 0.09	2290 ± 9	8.8 ± 0.74	2111 ± 60

Kinetic parameters derived from fitting with the Michaelis-Menten equation.
Data presented as parameter ± SE of parameter fit.

DMD Fast Forward. Published on January 18, 2011 as DOI: 10.1124/dmd.110.037036

Figure 1

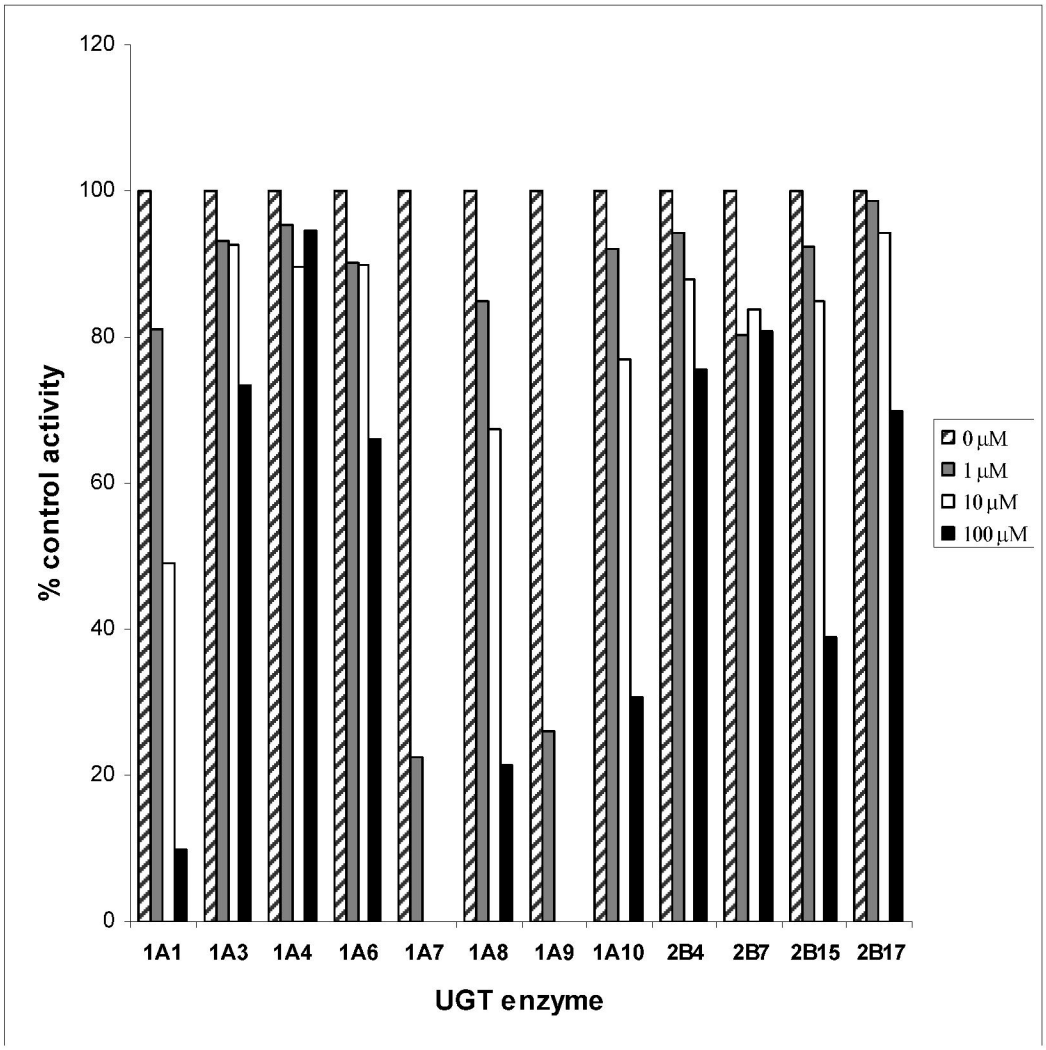

DMD Fast Forward. Published on January 18, 2011 as DOI: 10.1124/dmd.110.037036

Figure 2

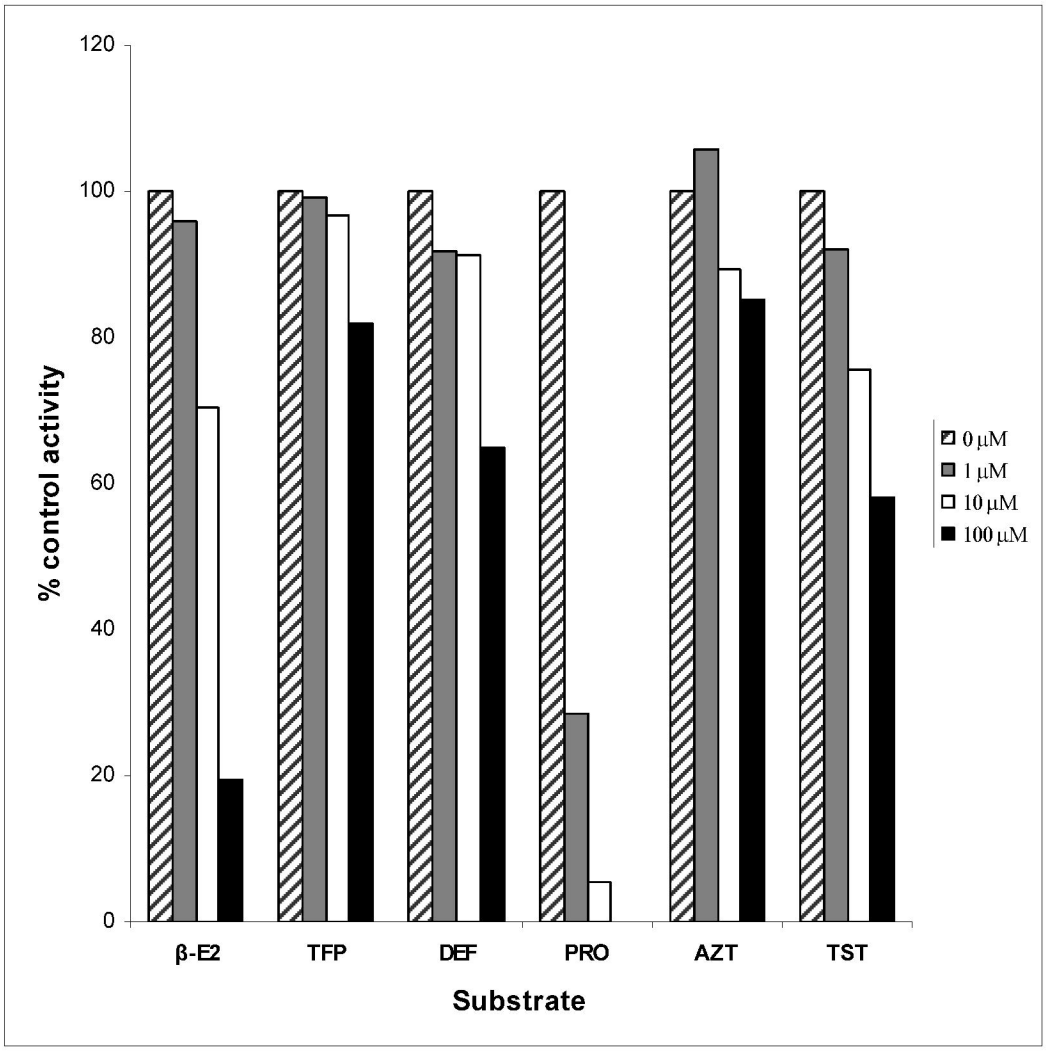

Figure 3

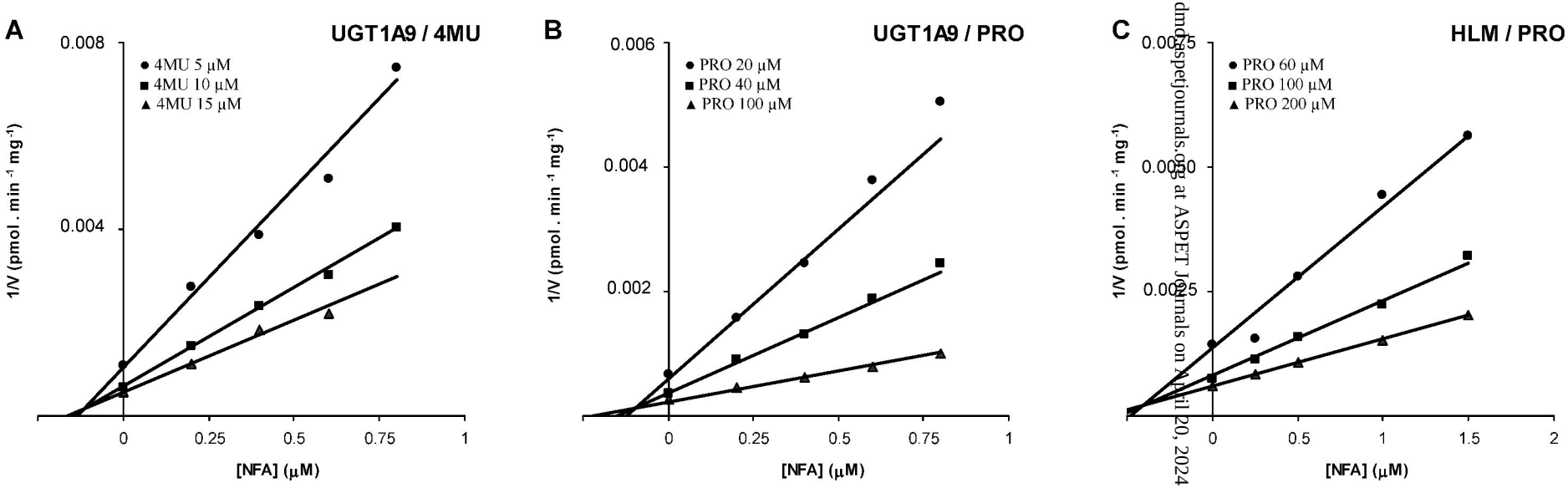

Figure 4

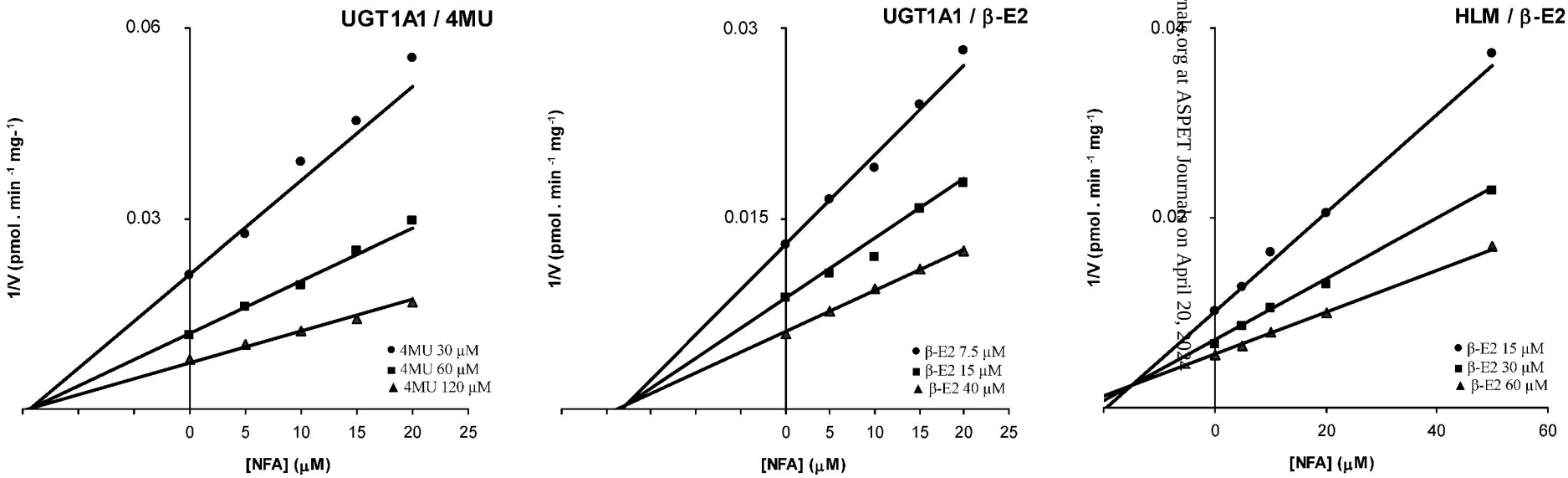

DMD Fast Forward. Published on January 18, 2011 as DOI: 10.1124/dmd.110.037036

Figure 5

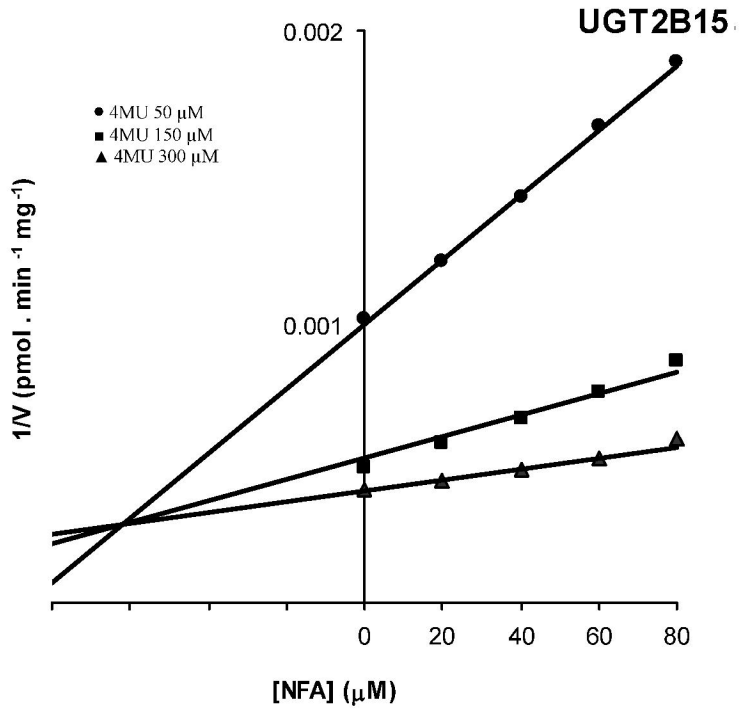

DMD Fast Forward. Published on January 18, 2011 as DOI: 10.1124/dmd.110.037036

Figure 6

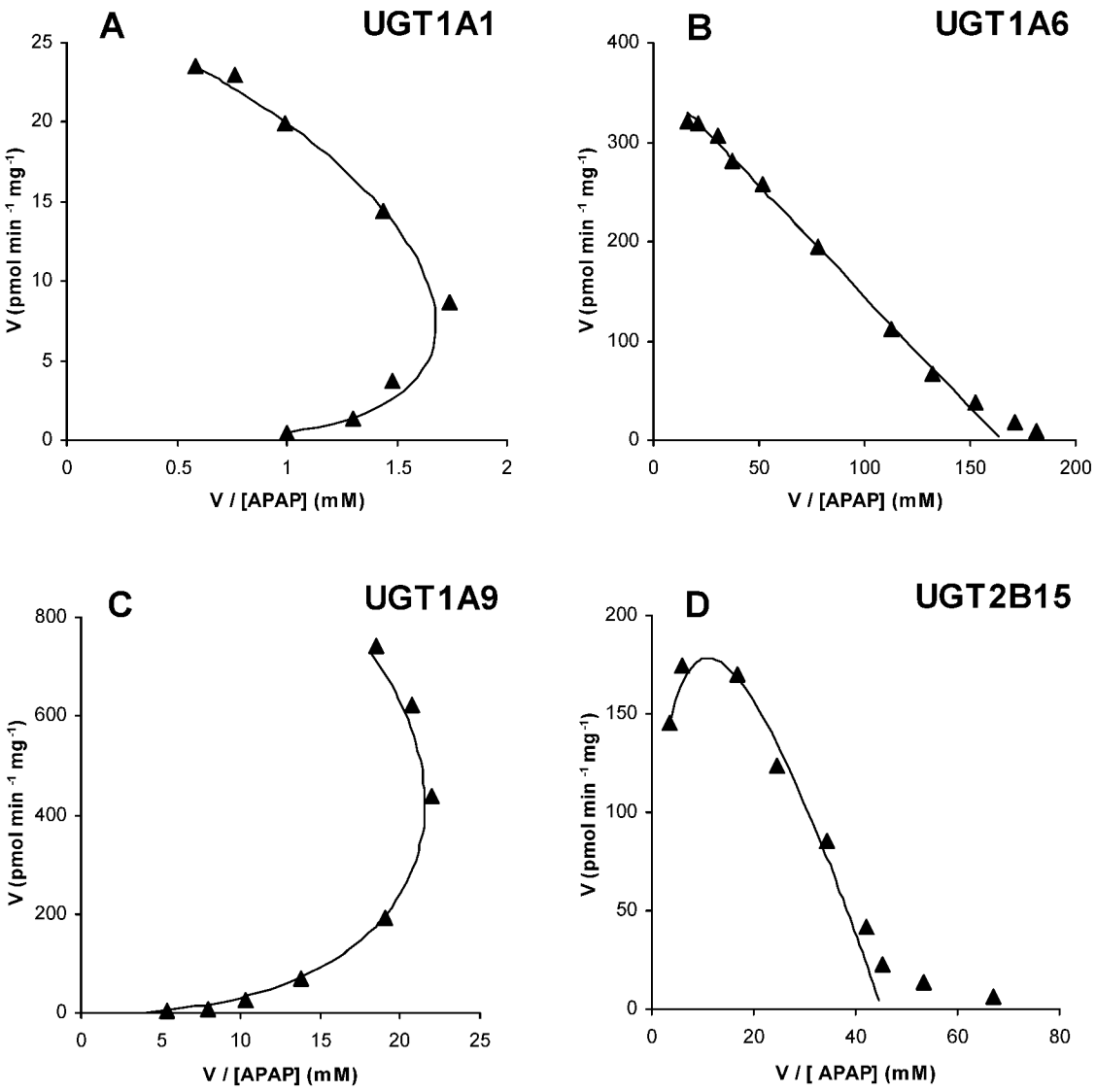

DMD Fast Forward. Published on January 18, 2011 as DOI: 10.1124/dmd.110.037036
This article has not been copyedited and formatted. The final version may differ from this version.

Figure 7

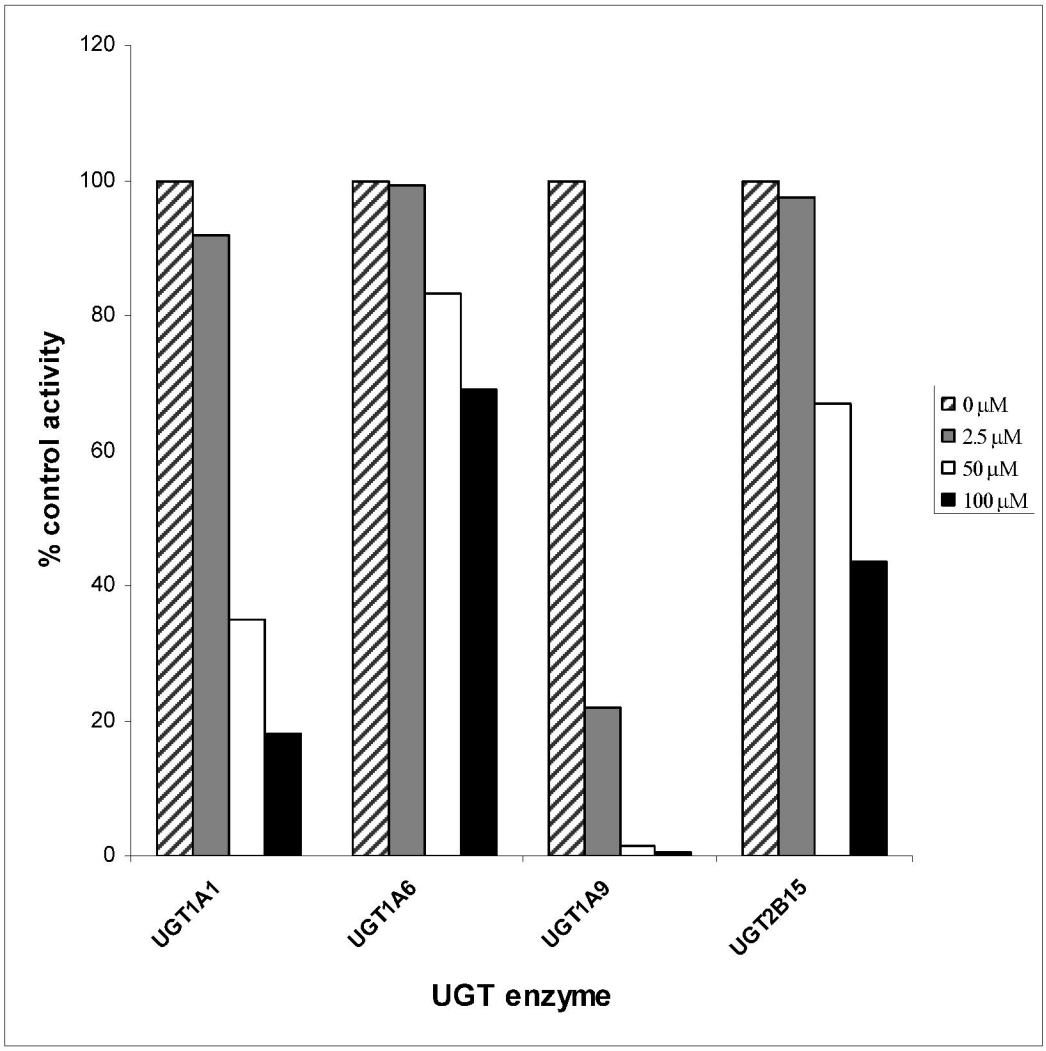

Figure 8